Intrarenal B Cell Cytokines Promote Transplant Fibrosis and Tubular Atrophy

Title
Intra-renal B cell cytokines promote transplant fibrosis and tubular atrophy

Author List
G.H. Tse[1]
C.J.C. Johnston[2]
D. Kluth[1]
M. Gray[1]
D. Gray[2]
J. Hughes[1]
L.P. Marson[1]

Department and Institution
1. Medical Research Council/University of Edinburgh Centre for Inflammation Research,
Queen's Medical Research Institute,
Edinburgh EH16 4TJ,
United Kingdom.

2. Institute of Immunology and Infection Research,
School of Biological Sciences,
University of Edinburgh,
Edinburgh EH9 3JT,
United Kingdom

Corresponding Author

Name:	George Tse
Email:	gtse@staffmail.ed.ac.uk, georgetse@doctors.org.uk
Mailing Address:	(Room W2.02) Medical Research Council/University of Edinburgh Centre for Inflammation Research, Queen's Medical Research Institute, Edinburgh EH16 4TJ, United Kingdom.
Telephone:	(+44) 131 242 6671
Fax:	(+44) 131 242 6578

Running Title
B-cells promote chronic allograft damage

Key Words
B cell, Chronic allograft damage, Mouse Model, Renal Transplant, Fibrosis

Abbreviations
CAD, Chronic Allograft Damage
TLT, Tertiary Lymphoid Tissue
IFTA, Interstitial Fibrosis and Tubular Atrophy

Abstract

Renal transplantation is the optimum treatment for end-stage renal failure. B cells have been identified in chronic allograft damage (CAD) and associated with the development of tertiary lymphoid tissue within the human renal allograft. We performed renal transplantation in mice to model CAD and identified B cells forming tertiary lymphoid tissue with germinal centres. Intra-allograft $B220^+$ B-cells comprised of IgM^{high} $CD23^-$ B cells, IgM^{lo} $CD23^+$ B cells and IgM^{lo} $CD23^-$ B cells with elevated expression of CD86. Depletion of B cells with anti-CD20 was associated with an improvement in CAD but only when administered after transplantation and not before. Isolated intra-allograft B cells were cultured and shown to synthesise multiple cytokines, the most abundant of these were GRO-α (CXCL1), RANTES (CCL5), IL-6 and MCP-1 (CCL2). Tubular loss was observed with T cell accumulation within the allograft and development of interstitial fibrosis, whilst type III collagen deposition was observed in areas of $F4/80^+$ macrophages and PDGFR-β^+ and $transgelin^+$ fibroblasts, all of which were reduced by B cell depletion. We have shown that intra-allograft B cells are key mediators of CAD. B cells possibly contribute to CAD by intra-allograft secretion of cytokines and chemokines.

Introduction

Renal transplantation is the optimum treatment for many patients with end-stage renal failure (1). A major challenge of renal transplantation is chronic allograft damage (CAD) characterized by interstitial fibrosis and tubular atrophy. The pathophysiology is poorly understood and multiple cell mediators and mechanisms are involved (2).

B cells have been identified in biopsies of renal transplants with stable function (3), in the context of acute rejection (4, 5), and chronic damage (6). However other studies have not correlated the presence of B cells to be detrimental (7), and B cells have been associated with the development of ectopic lymphoid tissue, also termed tertiary lymphoid tissue (TLT), within the human renal allograft (8). Although TLT in humans has been found in multiple chronic inflammatory disease states (9), the role of intra-allograft B cells and their significance have not been well explored (10).

The presence of B cells infiltrating inflammatory tissue in other models of disease has been associated with worse injury. Early depletion of B cells in myocardial infarction reduced the number of B cells recruited to the tissue and this was associated with significant improvement in post infarction cardiac function, furthermore recruitment of macrophages into the tissue and subsequent fibrosis were reduced (11). In a similar manner liver fibrosis was attenuated in mice deficient in intra-hepatic B cells (12), and CD19 deficient mice developed less Beomycin-induced pulmonary-fibrosis (13).

However the non-specific depletion of B-cells has been met with caution as the presence of regulatory B cells has been associated with protection from disease in some models (14, 15). Indeed a clinical study of B cell depletion as induction to renal transplantation was associated with a significant increase in acute rejection (16). There has been increasing interest in the functions of B cells beyond their role in antibody production, including cytokine-mediated effects in human disease (17, 18). In this report we have shown that intra-allograft B cells are key mediators of CAD and that B cells possibly contribute to CAD by intra-allograft secretion of cytokines and chemokines.

Materials and Methods

Mice and renal transplantation

Experiments performed under a UK Home Office Project Licence, granted under the Animal (Scientific Procedures) Act 1986 and approved by the University of Edinburgh ethical review committee. Eight-week old male C57BL/6 and BALB/c mice were obtained from Charles River, and C57BL/6^{BM12} colonies maintained in specific pathogen-free conditions in the Biological Research Resources Centre Edinburgh. Survival was greater than 80% for study groups. Anaesthesia was with intraperitoneal ketamine (75mg/kg) and medetomidine (1mg/kg), the donor kidney was perfused with cooled University of Wisconsin solution (Belzer Bridge to Life), the surgical technique was as previously reported (19). Renal transplantation was performed with a mean warm ischemic time of 30min. The donor ureter was anastomosed to recipient bladder. Anaesthesia was reversed with subcutaneous injection of atipamezole (1mg/kg) and buprenorphine (0.05mg/kg) for analgesia, with 1ml of 0.9% NaCl injected subcutaneously. The mouse was recovered and monitored in a warming cabinet at 28°C. A single intact native kidney was left *in situ* and the model was not transplant-dependent. To model CAD, heterotopic kidney transplantation was performed from a C57BL/6^{BM12} (H-2B^{BM12}) donor into a C57BL/6 (H-2B) recipient as previously described (19, 20). To model acute rejection a C57BL/6^{BM12} donor kidney was transplanted into a BALB/c (H-2d) recipient. For the isograft group C57Bl/6 kidneys were transplanted into litter mates.

B cell depletion

B cell depletion was performed by a single tail vein intravenous injection of 300µg anti-mouse CD20 mAb (18B12, IgGµ2a; Biogen Idec, San Diego, CA) in 200µl 0.9% NaCl, as described previously (21). Control placebo treated mice received anti-human anti-CD20 mAb (Rituximab; Biogen Idec).

Histology,

Immunohistochemistry, immunofluorescence methods and microscopy equipment are given in supplementary materials. Tubules within the cortex (x200 magnification, ten fields) were

counted using ImageJ software (Cell counter plugin; ImageJ 1.22o; National Institutes of Health, Bethesda, US). $B220^+$ B cell, $CD3^+$ T cells, $F4/80^+$ macrophages, picrosirius red, collagen III, SM22, PDGFR-β and α-SMA were expressed as average % area per high powered field (x200 magnification, ten fields) using a verified methodology of positive staining using Colour Range tool on Photoshop CS6 Extended (Version 13.0.6; Adobe Systems Europe) (22). Absolute numbers of $LYVE1^+$ lymphatic vessels and $PNAd^+$ high endothelial venules through the whole tissue section were expressed per mm^2 of the total tissue area calculated using ImageJ software. Pathological grading of T cell inflammation based on modified average T-score for each kidney (x200 magnification, ten fields, each given t-score of greatest degree per field) (23). T-score was calculated by T0 = no mononuclear cells in tubules, T1 = foci with 1-4 cells/tubular cross-section (or 10 tubular cells), T2 = foci with 5-10 cells/tubular cross-section, T3 = foci with >10 cells/tubular cross-section or the presence of at least two areas of tubular basement membrane destruction.

Kidney digestion

Single cell suspension from kidney digestion was prepared by mechanically fragmenting tissue using a No. 23 scalpel (Swann-Morton, UK) into IMDM (GIBCO, Life technologies, UK), 5% Fetal calf serum (Biosera Europe, France) and 1% Penicillin/Streptomycin (PAA Laboratories GmbH, Austria). The homogenate was centrifuged (5min, 300g) and re-suspended in 2ml Hanks Buffer (PAA Laboratories GmbH, Austria) containing 1.6mg/ml collagenase B (Roche Diagnostics GmbH, Mannheim, Germany) and 100g/ml DNAse I (Roche Diagnostics GmbH, Mannheim, Germany), and incubated at 37°C for 30min with occasional rotational mixing. The homogenate was passed through a 40µm cell strainer (BD Biosciences, USA) and cells were centrifuged (5min, 300g). Red blood cells were lysed by incubation on ice with red cell lysis buffer (Sigma Aldrich, USA) 10min.

Flow cytometry

For splenocyte and allograft lymphocyte flow cytometry cell analysis $1x10^6$ cells were stained for 30min at 4°C with primary antibodies given in supplementary materials. Cells were washed and DAPI added immediately before analysis using BD FACSDIVA version 6.1.3 on

a LSR Fortessa (BD Biosciences, USA). Analysis was gated on collecting 10,000 live B cell events. Post acquisition data analysis was performed using FlowJo version 10.6 (TreeStar Inc., USA). For peripheral flow cytometric analysis 12.5µl of peripheral blood was obtained by tail vein bleeding and added to 3.8% sodium citrate; aforementioned primary antibodies in 1% PBS were added and stained for 30min at 4°C before FACS lysing solution (BD Biosciences, San Jose, USA) was added before data acquisition along with CountBright Beads (Invitrogen, USA). See supplementary materials for cell sorting methods.

Circulating immunoglobulin titration

Blood was obtained by cardiac puncture with a 21G needle (Microvette 600, Germany) and serum was separated by centrifugation (10,000G, 5min) and frozen at -20°C till use. Determination of serum antibody concentrations was performed with a Luminex multiple analyte immunoglobulin profiling magnetic bead assay (Procartaplex, eBioscience, UK), prior to incubation with the bead assay serum was diluted 1:10,000 with universal buffer supplied within the assay kit. Luminex data acquisition was performed on a Bio-plex 200 system (Bio-Rad, USA) and analysis was performed using Bio-plex manager software (Version 6.0, Bio-Rad Labs Inc, USA).

Anti-donor antibody determination

Allospecific antibodies in sera of transplant recipients were assessed using indirect flow cytometry. Serum was assayed for anti-donor antibodies by their ability to bind C57BL/6^{BM12} splenocytes using flow cytometry. Splenocytes (0.5 x 10^6) were incubated in 50µL Dulbecco's PBS (PAA Laboratories GmbH, Austria) containing 1:20 recipient serum for 30min at 4°C followed by washes with PBS. Goat F(ab')2 polyclonal anti-IgG-FC-phycoerythrin (ABCAM, Cambridge, UK) was added and further incubated for 30min. Fluorescence analysis was determined by flow cytometry using a LSR Fortessa (Becton Dickinson, USA) and median fluorescence intensity measured post-acquisition using FlowJo (Tree Star Inc., USA). Conditions were performed in technical triplicates for samples derived from individual mice. In a similar manner auto-antibodies in the sera of transplant recipients were assessed using permeabilised cells. Splenocyte permeabilisation (Foxp3 Fixation/Permeabilization Set,

eBioscience) was performed prior to incubation with diluted recipient serum.

B Cell cytokine assay

Following FACS B cell isolation 2.5 x10^5 B cells were incubated in a 96-well plate in 250µl of IMDM GIBCO, Life technologies, UK), 10% FCS (Biosera Europe, France) and 1% Penicillin and Streptomycin (PAA Laboratories GmbH, Austria) for 72hr. In separate wells B-cells were stimulated with ionomycin 1µg/ml and PMA 20ng/ml or 2.5 x10^5 γ-irradiated C57BL/6^{BM12} splenocytes (Caesium-137, 30Gy). Determination of the presence of multiple cytokines was performed with a Luminex multiple analyte cytokine profiling magnetic bead assay (eBioscience, UK, or Bio-Rad, UK). Luminex data acquisition was performed on a Bio-plex 200 system (Bio-Rad, USA) and analysis was performed using Bio-plex manager software (Version 6.0, Bio-Rad Labs Inc, USA).

Statistical analysis

Data expressed as mean (SEM, standard error of the mean) unless otherwise stated. ANOVA (within groups and between multiple groups) with *post hoc* Bonferonni test, unpaired student's t-test (for parametric data-sets) and Mann-Whitney U tests (for non-parametric), were performed using Prism 5 for Mac OS X software (GraphPad Software Inc., La Jolla, Ca, USA). A p-value of less than 0.05 was considered significant.

Results

Mature B cells are recruited to the renal allograft

In CAD a progressive loss of tubules occurred over a twelve-week period, no difference in the number of healthy tubules between native kidneys and isograft kidneys was observed (Figure 1A, CAD vs Isograft ANOVA $p<0.0001$). The loss of nephron mass was accompanied by interstitial fibrosis, identified by picrosirius red staining of fibrillar collagen within the renal parenchyma. Following isograft transplantation minimal fibrosis developed with scarring being significantly greater in CAD kidneys (Figure 1B, CAD vs Isograft ANOVA $p<0.0001$). There was a progressive accumulation of $B220^+$ B cells within the allograft predominantly originating in a perivascular location, peaking at 12 weeks, whereas isograft kidneys were devoid of B cells (Figure 1B, ANOVA $p<0.0001$).

B cells form germinal centres and tertiary lymphoid tissue

Immunofluorescence confirmed B cells forming $GL7^+$ germinal centres and presence of $CD138^+$ plasma cells in 12-week allograft kidneys (Figure 1C). The development of TLT was further supported by the presence of $LYVE1^+$ lymphatics and $PNAd^+$ high endothelial venules (Figure 1C). Compartmentalization of intra-allograft B cells into TLT was suggested by the presence of B cells that were either $IgM^{high}\,CD23^-$, $IgM^{lo}\,CD23^+$ or $IgM^{lo}\,CD23^-$ (Figure 2A and 2B) suggesting some similarities with those found in spleen and found in a similar population distribution (Figure 2C). In addition a greater percentage of intra-allograft B cells expressed CD86 (B7-2) than naïve spleen B cells (Figure 2C, ANOVA $p<0.0001$), though there was no difference in CD80 expression between allograft B cells, naïve or allograft spleen B cells.

B cell depletion reduces interstitial fibrosis and tubular loss

To investigate whether the progression of CAD could be modified B cell depletion at 4 weeks after transplantation was performed. A monoclonal anti-CD20 approach was used to replicate human studies (16). This strategy effectively depleted peripheral blood $CD45.2^+$ $B220^+$ B cells compared to placebo anti-human anti-CD20 (Rituximab) treatment (Figure 3A). Peripheral blood B cells remained significantly suppressed for up to 4 weeks (Figure 3B, 8 weeks $p=0.004$, 12 weeks $p=0.0012$, student t-test) and intra-allograft B cells were also reduced

(Figure 3C, 8 and 12 weeks p=0.0001, U test). This intervention reduced interstitial fibrosis (Figure 4A and 4D, p=0.013, U test) and protected kidneys from tubular loss at 12 weeks (Figure 4B and 4D, p=0.013, U test) compared to placebo. Renal allograft expression of kidney injury molecule-1 (KIM-1) mRNA at 8 weeks was significantly reduced by B cell depletion at 4 weeks (Figure 4C, p=0.0173, U test). In comparison, B cell depletion 1 week prior to transplantation had no effect on the development of CAD (Figure S1, picrosirius red ANOVA p=0.0812, tubule count p=0.6521).

B cells depletion reduces formation of tertiary lymphoid tissue

B cell depletion at four weeks after transplantation inhibited the formation of $GL7^+$ germinal centres (Figure 5A, 8 weeks p=0.025 and 12 weeks p=0.0263, U test). Expansion of lymphatic vessels was noted between isograft and placebo treated allograft kidney at 12 weeks (Figure 5B, U test p=0.012), however B cell depletion had no significant effect on lymphatic numbers, though there was a trend towards reduction (Figure 5B). The ectopic development of $PNAd^+$ high endothelial venules, a component of TLT, was inhibited by B cell depletion (Figure 5C, 8 weeks p=0.044 and 12 weeks p=0.027, U test).

The effect of B cell depletion in CAD model is predominantly independent of antibody

Transplanting a C57BL/6 kidney into a BALB/c recipient is known to result in IgG donor-specific antibody and this was used as a positive control (Figure 6A and 6B, p<0.0001, ANOVA) (24). In CAD mice, serum concentration of IgM and total IgG were elevated at 4 weeks following allograft transplantation compared to naïve levels (Figure 6A). The elevated IgG isotype in CAD mice appeared to be of IgG1 and IgG3 subclass, IgG2a concentration was not elevated in C57BL6 recipients; however IgG1, IgG2a and IgG3 were elevated in BALB/c recipients (Figure S2). No IgG reactivity was observed against fresh $C57BL/6^{BM12}$ splenocytes in serum from C57BL/6 recipients, compared to a significant increase in the median fluorescence intensity (MFI) cell surface IgG binding following incubation with serum from BALB/c recipients (Figure 6B, p<0.0001, ANOVA). To investigate auto-antibody generation, $C57BL/6^{BM12}$ splenocytes were permeabilised prior to incubation with serum. Although an increase in MFI of IgG was observed in CAD mice compared to with naïve

C57BL serum, B cell depletion after transplantation had no affect on the presence of auto-reactive IgG (data not shown). IgG was apparent in the allograft tissue (Figure 6C), however IgM did not appear to be present within the allograft other than that expressed on the surface of B cells. B cell depletion by anti-CD20 did not reduce the amount of IgG in the CAD kidney either at 8 or 12 weeks post transplantation (Figure 6C, 8 weeks p=0.4848 and 12 weeks p=0.2403, U test). Lastly the complement split product C4d was not detected in rejecting allografts further suggesting that antibody-mediated rejection is not involved in this model of CAD. Glomerulopathy was not a feature, with normal glomeruli demonstrated in the presence of IFTA (Figure 4D).

T cell accumulation is reduced by B cell depletion

T cells were identified in perivascular regions as well as dispersed throughout the kidney parenchyma where they infiltrated glomeruli and tubules (Figure 7A). B cell depletion at four weeks after transplantation significantly reduced T cell density (Figure 7B, 8 weeks p=0.0052 and 12 weeks p=0.0002, U test), and the T-score (reflecting the level of pathological T cell-mediated injurious tubulitis) at 8 weeks (Figure 7B, 8 weeks p=0.045, U test). T cells could be identified crossing the basement membrane of tubules and invading renal tubules on transmission electron microscopy (Figure 7C). However few $GR1^+$ neutrophils were identified in the allograft and B cell depletion had no effect on their presence (Figure S3, 8 weeks p=0.2365 and 12 weeks p=0.4212, U test).

To identify the mechanism of T cell recruitment we isolated intra-allograft B cells from CAD kidneys at 4 weeks following transplantation. *Ex vivo* culture revealed B cells were activated to synthesize T cell chemokines, including GRO-α (CXCL1), RANTES (CCL5) and IP-10 (CXCL10) (Fig 8A, p=0.0035, p=0.0005, p=0.0093 respectively, ANOVA). Generation of these chemokines was not dependent on re-stimulation and levels were significantly higher than produced by naive B cells stimulated by ionomycin and phorbitol myrisate acetate. Isolated intra-allograft B cells also secreted multiple pro-inflammatory cytokines, including IL-6, IL-18, and TNF-α (Figure 8A, p<0.001, ANOVA). In addition IL-10 was assayed but was not detected in stimulated B cell supernatant (data not shown). To confirm the generation of

these cytokines *in vivo* by B cells, intra-allograft B cells were sorted into pure $CD45.2^+$ $B220^+$ populations; mRNA was immediately isolated and analyzed for the most abundantly expressed cytokines (Figure 8B).

Reduced fibrosis is associated with lower monocyte and fibroblast density

Type III collagen was detected in this model of CAD (Figure 9A). Late B cell depletion reduced type III collagen expression in the allograft kidney at both eight and twelve weeks (Figure 9B, both $p<0.0001$, U test), in keeping with reduced picrosirius red staining (Figure 4A). Intra-allograft $F4/80^+$ cells were reduced by late B cell depletion after transplantation (Figure 9B, 8 weeks $p=0.0007$ and 12 weeks $p<0.0001$, U test). Interestingly there was no difference in $\alpha\text{-SMA}^+$ myofibroblasts between placebo and B cell depletion (Figure 9B, 8 weeks $p=0.25$ and 12 weeks $p=0.82$, U test); α-SMA was restricted to intra-renal vessels and was not identified in proximity to type III collagen on serial sections (Figure 9A). Additionally the level of transgelin (Figure 9B, 12 weeks $p<0.0001$, U test) and PDGFR-β expression (Figure 9B, 8 weeks $p=0.420$ and 12 weeks $p<0.0001$, U test) were significantly reduced in B cell depletion and followed the same pattern as type III collagen in the renal parenchyma (Figure 9A).

The supernatant of *ex vivo* cultured isolated intra-allograft B cells was analysed to explore the role of activated B cells in fibrosis and significant levels of monocyte cytokines MCP-1 (CCL2), MCP-3 (CCL7) and MIP-2 (CXCL2) were found (Figure 10A, $p=0.0401$, $p=0.0334$, $p=0.0002$ respectively, ANOVA). Furthermore stimulation of B cells with irradiated $C57BL/6^{BM12}$ splenocytes stimulated the synthesis of TGF-β1, MIP-1α and MIP-1β (Figure 10A, $p=0.0074$, $p=0.0232$, $p=0.0298$ respectively, ANOVA); mRNA expression of the most abundant cytokines was confirmed in freshly isolated B cells (Figure 10B).

Discussion

In this study we have demonstrated a key function of intra-allograft B cells to be the secretion of cytokines. The depletion of intra-allograft B cells reduced T cell accumulation and fibroblastic cells that mediate interstitial fibrosis. In addition, intra-allograft B cells expressed the co-stimulatory molecule, CD86, as a marker of an antigen-presenting cell. CD86 expression by antigen presenting cells play an important role in co-stimulation for T cell activation (25). Recent study of acute rejection in human renal transplant biopsies correlated the presence of $CD20^+$ B cell clusters with steroid resistant T cell mediated cellular rejection (5); intriguingly B cell clusters have also been identified in chronically rejected transplants (26, 27), and in relation to lymphatic neoangiogenesis (28), as such, much is still unknown about the role of intra-allograft B cells in transplantation. In this model B cells appear as nodular infiltrates in a perivascular distribution, mimicking that described in human studies (3, 26). These results are in agreement with previous studies using this donor and recipient combination, modeling rejection in both cardiac (29) and renal transplantation (20). Furthermore the compartmentalization of intra-allograft B cells into TLT was suggested by the presence of B cells that expressed surface markers which had some similarities with those found in spleen (30).

Type III collagen is a fibrillar protein that is synthesized in inflammation and present in chronic rejection of human renal allografts (31), and was detected in this model. Despite the association between intra-allograft B cells and interstitial fibrosis, this was not mediated through α-SMA-expressing myofibroblasts, although the expression of α-SMA is associated with a great degree of variability (32, 33). Other mechanisms promoting fibrosis were therefore examined: activated pericytes express platelet derived growth factor receptor-β (PDGFR-β) and can differentiate into fibroblasts (34). Transgelin is an actin stress fibre-associated protein and an early marker of smooth muscle cell differentiation, and is associated with renal fibroblast activation (35). Both transgelin and PDGFR-β, which may be alternative markers of fibroblast activation, were expressed in areas of tubular atrophy and we speculate that B cells could potentially drive fibrocyte or fibroblast activation through these mechanisms.

Increasingly it is recognized that B cells may be an important source of pro-

inflammatory and anti-inflammatory cytokines (18). We found that intra-allograft B cells synthesise GRO-α, IL-6, RANTES, CXCL-10 and MCP-1 in the greatest abundance and that B cells can be further induced by re-stimulation with donor antigens. The most highly synthesized of these cytokines was GRO-α which has been reported to be a major stimulus for neutrophil chemotaxis (36), however there were very few neutrophils present in the allograft tissue, suggesting an alternative role for this cytokine. Recently GRO-α has been shown to play a role in angiogenesis (37), therefore it is hypothesized that GRO-α plays a role in TLT development as B cell depletion inhibited the formation of germinal centres, high endothelial venules and lymphatic expansion. The presence of B cells at sites of inflammation has been associated with fibrosis. Specifically following myocardial infarction B cells induced local macrophage recruitment through MCP-3 (CCL7) production (11), similarly we found B cells synthesise this cytokine within the allograft however to a lesser degree than MCP-1 (CCL2).

An interesting feature of this model of CAD is the generation of IgG auto-antibodies that appear to be IgG1 or IgG3 isotypes. Following C57BL/6^{BM12} cardiac transplantation in C57BL/6 recipients IgG auto-antibodies have been observed (38). The IgG1 isotype is not capable of fixing complement and in a cardiac allograft model this isotype was not capable of mediating rejection, however IgG1 may stimulate endothelial cells to produce CXCL1 and CCL2 which are potent chemo-attractants to neutrophils and macrophages (39). Potentially intra-allograft B cells promote fibrosis by recruiting monocytes into the allograft, thereby supporting macrophage-mediated fibrosis or directly activate profibrotic cells through TGF-β1. Intriguingly in patients that develop chronic renal transplant rejection *de* novo auto-antibodies have been detected (40). Serum IgM was attenuated in B cell depleted animals however no significant change in isotype switched Ig or IgG deposition in the allograft was found. It is possible that even if the antibodies were not complement fixing they may still play a role in CAD by promoting Fc-receptor mediated functions in cells such as macrophages.

B cell depletion was performed by monoclonal anti-CD20 antibody depletion, with the human counterpart that has been widely used in human disease and its safety profile proven. However when used in depletion prior to renal transplantation this was shown to significantly increase acute rejection (16). Some evidence in human studies supports the hypothesis that

B cell depletion in late allograft failure may be beneficial beyond targeting antibody-mediated rejection. In small series and case studies Rituximab, in addition to other immuno-modulatory therapies, has been administered to patients with late allograft failure with improvement or return of function without any change in circulating DSA levels (41-44). One might speculate that this protection is against intra-graft B cell production of the cytokines as described in our model.

Another issue raised in this study is that depletion of B cells prior to transplantation had no affect on CAD whereas depletion at four weeks post transplantation inhibited CAD. Paradoxically in patients with long-term tolerance a B cell specific signature has been identified (45), however this was in peripheral blood samples. The allograft B cells in this study did not produce interleukin-10, this argues against an anti-inflammatory role for them. TGF β was produced by allograft B cells and has been associated with tolerance (46), however it also well characterized as a profibrotic cytokine (47). Thus 'regulatory B cells' are under investigation and this highlights the complex nature of B cell compartments and the challenge in determining their modes of action.

Here we have shown that intra-allograft B cells are a major source of cytokines that may orchestrate T cell and monocyte recruitment and thus contribute to chronic damage and scarring in the renal allograft. These findings suggest that intra-allograft B cells *per se* and their cytokine and chemokine pathways represent potential novel therapeutic target for therapy in human renal transplantation.

Acknowledgements

This work was funded through a Kidney Research UK clinical training fellowship and a small research grant from The Royal College of Surgeons of Edinburgh. We wish to thank Spike Clay and Gary Borthwick for their assistance with animal surgery and welfare. mAb Anti-CD20 was kindly supplied by Dr Jeff Browning at Biogen Idec (Boston, USA).

Disclosures

The authors of this manuscript have no conflicts of interest to disclose as described by the *American Journal of Transplantation*.

Figure Legends

Figure 1: B cells accumulate within transplanted kidneys undergoing chronic allograft damage (CAD)(C57BL/6^{BM12}⇨C57BL/6).

(A) Representative histology of paraffin-embedded allograft transplant kidney sections. Haemotoxylin and eosin for tissue architecture, collagen with picrosirius red (red), B220^{+} B cells (brown). (B) Quantification of the number of tubules, density of collagen and B cells in transplanted kidneys. Ten micrographs at x200 magnification were analyzed (n=6 mean (SEM), ANOVA and Bonferonni *post hoc* between groups at time points. *p<0.05; **p<0.01). (C) Definition of CAD B cell infiltrates 12 weeks post transplantation in immunofluorescent micrographs identifying GL7^{+} germinal centres and CD138^{+} plasma cells, and tertiary lymphoid tissue development with PNAd^{+} high endothelial venules and LYVE1^{+} lymphatic vessels.

Figure 2: The phenotype of allograft (C57BL/6^{BM12}⇨C57BL/6) B cells by flow cytometry.

(A) Gating of B cells from allograft kidney digest. Intra-allograft B cells isolated following allograft kidney digestion then B220^{+} magnetic bead enrichment prior to fluorescence activated cell sorting by B220^{+} CD45.2^{+} DAPI^{-} for mRNA extraction and cell culture experiments. (B) CAD intra-allograft B cell phenotype were analysed on flow cytometry and compared to naive spleen B cells. (C) Frequency of gated B cells (n=6, mean (SEM), ANOVA and Bonferonni *post hoc* between groups. **p<0.01).

Figure 3: Anti-CD20 after transplantation depletes intra-renal B cells in chronic allograft damage (C57BL/6^{BM12}⇨C57BL/6)

(A) Flow cytometry gating of blood B cells prior to and following anti-mouse anti-CD20 or anti-human anti-CD20 (Rituximab). (B) Absolute count of blood B cells were determined in mice treated prior to, or 4 weeks after, transplantation (n=6, mean (SEM), ANOVA and Bonferonni *post hoc* between groups at single time points. **p<0.01; ***p<0.001). (C) Quantification of the immunohistochemistry micrographs of allograft density of B220^{+} B cells following anti-mouse anti-CD20 or anti-human anti-CD20 (Rituximab). Ten micrographs at x200

magnification were analyzed (n=6 mean (SEM), Mann-Whitney U test. ***p<0.001).

Figure 4: B cell depletion reduces chronic allograft damage (C57BL/6^{BM12}⇨C57BL/6).

(A) Quantification of allograft density of collagen following picrosirius red staining following anti-mouse anti-CD20 or anti-human anti-CD20 (Rituximab). (B) Quantification of the number of tubules by haemotoxylin and eosin staining following treatment. Ten micrographs at x200 magnification were analyzed (n=6, mean (SEM), Mann-Whitney U test between groups at single time points. *p<0.05; **p<0.01). (C) Allografts at 8 weeks after transplantation from mice depleted at 4 weeks of B cells had a decreased expression of CD20 and Kim-1 mRNA (n=8, assay in triplicate, mean (SEM), Mann-Whitney U test. *p<0.05). (D) Representative histology of paraffin-embedded transplant kidney sections. Fibrosis identified by collagen with picrosirius red, tubular atrophy demonstrated in untreated and placebo treated tissue.

Figure 5: Reduction in tertiary lymphoid tissue development.

(**A**) Representative immunohistochemistry of GL7^{+} germinal centres (brown) counted per total tissue area section. (**B**) Absolute numbers of LYVE1^{+} lymphatic vessels (brown) per total tissue area section. (**C**) Absolute numbers of PNAd^{+} high endothelial venules (brown) per total tissue area section in anti-CD20 or placebo (Rituximab) treated allograft kidneys (n=6, mean (SEM), Mann-Whitney U test. *p<0.05).

Figure 6: CAD is not primarily mediated by donor-specific immunoglobulin

C57BL/6^{BM12} donor kidneys transplanted in to **C57BL/6 allograft** recipients (C57BL/6^{BM12}⇨C57BL/6) or **BALBc allograft** recipients (C57BL/6^{BM12}⇨BALB/c). (A) Serum concentrations of IgM and total IgG from naïve and transplant recipient mice were measured (see supplemental table 1 for absolute values)(n=5, assay in duplicate, mean (SEM), ANOVA and Bonferonni *post hoc* between groups. *p<0.05; **p<0.01; ♯p<0.001 against all groups). (B) Flow cytometry of live splenocytes incubated with transplant recipient serum to detect donor-specific IgG, quantification by median fluorescent intensity (n=6, assay in triplicate, error bars median and interquartile-range, ANOVA and Bonferonni *post hoc* between groups. ***p<0.001). (C) Intra-allograft IgG content with representative immunofluorescence

comparing naïve kidney and of CAD allograft 12 weeks post-transplantation demonstrating deposited IgG (green) and B cells bearing IgG. Quantification of IgG+ micrographs following treatment (n=6, mean ± SEM, Mann-Whitney U test, N.S.).

Figure 7: B cell depletion reduces T cell accumulation.

(A) Representative immunohistochemistry of $CD3^+$ infiltrating T cells (brown). T cells identified invading glomeruli (hollow arrows) and tubules (block arrows). (B) Quantification of the immunohistochemistry micrographs to determine allograft density of $CD3^+$ T cells in anti-CD20 or placebo treated (Rituximab). Pathological grading (T-score) of allografts treated at four weeks. Ten micrographs at x200 magnification were analyzed (n=6, mean (SEM), Mann-Whitney U test. *p<0.05; **p<0.01; ***p<0.001). (C) Transmission electron microscopy image of CAD kidney at 8 weeks post transplantation. T cell can be identified breaching the basement membrane and invading the renal tubule.

Figure 8: B cells secrete fibrosis related cytokines.

(A) Cytokine supernatant assay of isolated allograft ($C57BL/6^{BM12}$⇨C57BL/6) B cells cultured for 72 hours alone or ionomycin (Ion.) and phorbitol mysirate (PMA) and compared to stimulated naïve B cells (n=6, mean (SEM), ANOVA and Bonferonni *post hoc* between pairs of groups. *p<0.05; **p<0.01; ***p<0.001). (B) Comparative quantification of mRNA fold difference by qRT-PCR in isolated allograft B cells compared to naïve spleen B cells, genes of interest normalized to two genes with 18s represented (n=8, assay in triplicate).

Figure 9: Reduced fibrosis is associated with fewer macrophage and fibroblasts in the allograft (C57BL/6^{BM12}⇨C57BL/6).

(A) Representative immunohistochemistry of serial sections for type III collagen, F4/80, α-Smooth Muscle Actin (α-SMA), SM22 (transgelin) and platelet derived growth factor receptor-β (PDGFR-β). (B) Quantification of type III collagen, $F4/80^+$ mononuclear cell infiltration, presence of $\alpha\text{-SMA}^+$ myofibroblast, $PDGFR\text{-}\beta^+$ or $transgelin^+$ fibroblast-like cells in anti-CD20 or placebo (Rituximab) treated allograft treated at four weeks. Ten micrographs at x200 magnification were analyzed (n=6, mean (SEM), Mann-Whitney U test. ***p<0.001).

Figure 10: B cells secrete profibrotic cytokines.

(A) Cytokine supernatant assay of isolated allograft (C57BL/6^{BM12}⇨C57BL/6) B cells cultured for 72 hours alone in media or ionomycin (Ion.) and phorbitol mysirate (PMA) or with γ-irradiated C57BL/6^{BM12} splenocytes and compared to stimulated naïve B cells (n=6-8, assay in duplicate, mean (SEM), ANOVA and Bonferonni *post hoc* between pairs of groups. *p<0.05; **p<0.01). (B) Comparative quantification of mRNA fold difference by qRT-PCR in isolated allograft B cells compared to naïve spleen B cells, genes of interest normalized to two genes with 18s represented (n=8, assay in triplicate).

Figure S1: CAD (C57BL/6^{BM12}⇨C57BL/6) is not altered by B cell depletion prior to transplantation.

Quantification of allograft density of collagen following picrosirius red staining following anti-mouse anti-CD20 or anti-human anti-CD20 (Rituximab) 1 week prior to transplantation. Quantification of the number of tubules by haemotoxylin and eosin staining following treatment. Ten micrographs at x200 magnification were analyzed (n=6, mean (SEM), ANOVA and Bonferonni *post hoc* between pairs of groups. N.S.).

Figure S2: Serum concentration of IgG subclasses.

C57BL/6^{BM12} donor kidneys transplanted in to C57BL/6 allograft recipients (C57BL/6^{BM12}⇨C57BL/6) or BALBc allograft recipients (C57BL/6^{BM12}⇨BALB/c). Serum concentration of IgG subclasses from naïve and transplant recipient mice were measured (see **Supplemental Table S1** for absolute values)(n=5, assay in duplicate, mean (SEM), ANOVA and Bonferonni *post hoc* between pairs of groups. *p<0.05; **p<0.01; ♯p<0.001 against all groups).

Figure S3: B cell depletion did not effect allograft (C57BL/6^{BM12}⇨C57BL/6) neutrophil infiltration.

(A) Intra-allograft Gr1^{+} neutrophils (hollow arrows) identified on immunohistochemistry (brown). (B). Quantification of the immunohistochemistry micrographs of allograft Gr1^{+}

neutrophils following treatment, ten micrographs at x200 magnification were analyzed (n=6, mean (SEM), ANOVA followed by Mann-Whitney U test. N.S).

Supporting Information

Additional Supporting Information may be found in the online version of this article.

Supplementary Materials

Figure S1: CAD (C57BL/6^{BM12}⇨C57BL/6) is not altered by B cell depletion prior to transplantation.

Figure S2: Serum concentration of IgG subclasses

Figure S3: B cell depletion did not effect allograft (C57BL/6^{BM12}⇨C57BL/6) neutrophil infiltration

Table S1: Serum isotype

References

1. Wolfe RA, Ashby VB, Milford EL, Ojo AO, Ettenger RE, Agodoa LYC et al. Comparison of mortality in all patients on dialysis, patients on dialysis awaiting transplantation, and recipients of a first cadaveric transplant. N Engl J Med 1999;341:1725-1730.
2. Nankivell BJ, Alexander SI. Rejection of the kidney allograft. N Engl J Med 2010;363:1451-1462.
3. Mengel M, Gwinner W, Schwarz A, Bajeski R, Franz I, Bröcker V et al. Infiltrates in protocol biopsies from renal allografts. Am J Transplant 2007;7:356-365.
4. Kayler LK, Lakkis FG, Morgan C, Basu A, Blisard D, Tan HP et al. Acute cellular rejection with CD20-positive lymphoid clusters in kidney transplant patients following lymphocyte depletion. Am J Transplant 2007;7:949-954.
5. Zarkhin V, Kambham N, Li L, Kwok S, Hsieh SC, Salvatierra O et al. Characterization of intra-graft B cells during renal allograft rejection. Kidney Int 2008;74:664-673.
6. Adair A, Mitchell DR, Kipari T, Qi F, Bellamy CO, Robertson F et al. Peritubular capillary rarefaction and lymphangiogenesis in chronic allograft failure. Transplantation 2007;83:1542-1550.
7. Doria C, di Francesco F, Ramirez CB, Frank A, Iaria M, Francos G et al. The presence of B-cell nodules does not necessarily portend a less favorable outcome to therapy in patients with acute cellular rejection of a renal allograft. Transplant Proc 2006;38:3441-3444.
8. Thaunat O, Field AC, Dai J, Louedec L, Patey N, Bloch MF et al. Lymphoid neogenesis in chronic rejection: evidence for a local humoral alloimmune response. Proc Natl Acad Sci U S A 2005;102:14723-14728.
9. Marinkovic T, Garin A, Yokota Y, Fu Y-X, Ruddle NH, Furtado GC et al. Interaction of mature CD3+CD4+ T cells with dendritic cells triggers the development of tertiary lymphoid structures in the thyroid. J Clin Invest 2006;116:2622-2632.10.
10. Segerer S, Schlondorff D. B cells and tertiary lymphoid organs in renal inflammation. Kidney Int 2008;73:533-537.
11. Zouggari Y, Ait-Oufella H, Bonnin P, Simon T, Sage AP, Guerin C et al. B lymphocytes trigger monocyte mobilization and impair heart function after acute myocardial infarction. Nature Med 2013;19:1273-1280.
12. Novobrantseva TI, Majeau GR, Amatucci A, Kogan S, Brenner I, Casola S et al. Attenuated liver fibrosis in the absence of B cells. J Clin Invest 2005;115:3072-3082.
13. Komura K, Yanaba K, Horikawa M, Ogawa F, Fujimoto M, Tedder TF et al. CD19 regulates the development of bleomycin-induced pulmonary fibrosis in a mouse model. Arthritis Rheum 2008;58:3574-3584.
14. Gray M, Miles K, Salter D, Gray D, Savill J. Apoptotic cells protect mice from autoimmune inflammation by the induction of regulatory B cells. Proc Natl Acad Sci U S A 2007;104:14080-14085.

15. Matsushita T, Yanaba K, Bouaziz J-D, Fujimoto M, Tedder TF. Regulatory B cells inhibit EAE initiation in mice while other B cells promote disease progression. J Clin Invest 2008;118:3420-3430.
16. Clatworthy MR, Watson CJ, Plotnek G, Bardsley V, Chaudhry AN, Bradley JA et al. B-cell-depleting induction therapy and acute cellular rejection. N Engl J Med 2009;360:2683-2685.
17. Barr TA, Shen P, Brown S, Lampropoulou V, Roch T, Lawrie S et al. B cell depletion therapy ameliorates autoimmune disease through ablation of IL-6 producing B cells. J Exp Med 2012;209:1001-1010.
18. Lund FE. Cytokine-producing B lymphocytes – key regulators of immunity. Curr Opin Immunol 2008;20:332-338.
19. Tse GH, Hesketh EE, Clay M, Borthwick G, Hughes J, Marson LP. Mouse kidney transplantation: Models of allograft rejection. J Vis Exp 2014;92:e52163.
20. Dang Z, Mackinnon A, Marson LP, Sethi T. Tubular atrophy and interstitial fibrosis after renal transplantation is dependent on galectin-3. Transplantation 2012;93:477-484.
21. Hamel KM, Cao Y, Ashaye S, Wang Y, Dunn R, Kehry MR et al. B cell depletion enhances T regulatory cell activity essential in the suppression of arthritis. J Immunol 2011;187:4900-4906.
22. Tse GH, Marson LP. A comparative study of 2 computer-assisted methods of quantifying brightfield microscopy images. Appl Immunohistochem Mol Morphol 2013;21:464-470.
23. Sis B, Mengel M, Haas M, Colvin RB, Halloran PF, Racusen LC et al. Banff '09 Meeting Report: Antibody Mediated Graft Deterioration and Implementation of Banff Working Groups. Am J Transplant 2010;10:464-471.
24. Coffman T, Geier S, Ibrahim S, Griffiths R, Spurney R, Smithies O et al. Improved renal function in mouse kidney allografts lacking MHC class I antigens. J Immunol 1993;151:425-435.
25. Greenwald RJ, Freeman GJ, Sharpe AH. The B7 family revisited. Annu Rev Immunol 2005;23:515-548.
26. Thaunat O, Patey N, Caligiuri G, Gautreau C, Mamani-Matsuda M, Mekki Y et al. Chronic rejection triggers the development of an aggressive intragraft immune response through recapitulation of lymphoid organogenesis. J Immunol 2010;185:717-728.
27. Einecke G, Reeve J, Mengel M, Sis B, Bunnag S, Mueller TF et al. Expression of B cell and immunoglobulin transcripts is a feature of inflammation in late allografts. Am J Transplant 2008;8:1434-1443.
28. Kerjaschki D, Regele H, Mooseberger I, Nagy-Bojarszki K, Watschinger B, Soleiman A et al. Lymphatic neoangiogenesis in human kidney transplants is associated with immunologically active lymphocytic infiltrates. J Am Soc Nephrol 2004;15:603-612.

29. Motallebzadeh R, Rehakova S, Conlon TM, Win TS, Callaghan CJ, Goddard M et al. Blocking lymphotoxin signaling abrogates the development of ectopic lymphoid tissue within cardiac allografts and inhibits effector antibody responses. FASEB J 2012;26:51-62.
30. Oliver AM, Martin F, Gartland GL, Carter RH, Kearney JF. Marginal zone B cells exhibit unique activation, proliferative and immunoglobulin secretory responses. Eur J Immunol 1997;27:2366-2374.
31. Farris AB, Colvin RB. Renal interstitial fibrosis: mechanisms and evaluation. Curr Opin Nephrol Hypertens 2012;21:289-300.
32. Okada H, Ban S, Nagao S, Takahashi H, Suzuki H, Neilson EG. Progressive renal fibrosis in murine polycystic kidney disease: An immunohistochemical observation. Kidney Int 2000;58:587-597.
33. Duffield JS. Cellular and molecular mechanisms in kidney fibrosis. J Clin Invest 2014;124:2299-2306.
34. Henderson NC, Arnold TD, Katamura Y, Giacomini MM, Rodriguez JD, McCarty JH et al. Targeting of [alpha]v integrin identifies a core molecular pathway that regulates fibrosis in several organs. Nature Med 2013;19:1617-1624.
35. Karagianni F, Prakoura N, Kaltsa G, Politis P, Arvaniti E, Kaltezioti V et al. Transgelin up-regulation in obstructive nephropathy. PLoS ONE 2013;8:e66887.
36. Hammond ME, Lapointe GR, Feucht PH, Hilt S, Gallegos CA, Gordon CA et al. IL-8 induces neutrophil chemotaxis predominantly via type I IL-8 receptors. J Immunol 1995;155:1428-1433.
37. Miyake M, Goodison S, Urquidi V, Gomes Giacoia E, Rosser CJ. Expression of CXCL1 in human endothelial cells induces angiogenesis through the CXCR2 receptor and the ERK1/2 and EGF pathways. Lab Invest 2013;93:768-778.
38. Win TS, Rehakova S, Negus MC, Saeb-Parsy K, Goddard M, Conlon TM et al. Donor CD4 T cells contribute to cardiac allograft vasculopathy by providing help for autoantibody production. Circ Heart Fail 2009;2:361-369.
39. Rahimi S, Qian Z, Layton J, Fox-Talbot K, Baldwin WM, Wasowska BA. Non-Complement- and Complement-Activating Antibodies Synergize to Cause Rejection of Cardiac Allografts. Am J Transplant 2004;4:326-334.
40. Porcheray F, DeVito J, Yeap BY, Xue L, Dargon I, Paine R et al. Chronic humoral rejection of human kidney allografts associates with broad autoantibody responses. Transplantation 2010;89:1239-1246.
41. Faguer S, Kamar N, Guilbeaud-Frugier C, Fort M, Modesto A, Mari A et al. Rituximab therapy for acute humoral rejection after kidney transplantation. Transplantation 2007;83:1277-1280.
42. Billing H, Rieger S, Ovens J, Susal C, Melk A, Waldherr R et al. Successful treatment of chronic antibody-mediated rejection with IVIG and rituximab in pediatric renal transplant recipients. Transplantation 2008;86:1214-1221.

43. Tanriover B, Mejia A, Weinstein J, Foster SV, Ghalib R, Mubarak A et al. Analysis of kidney function and biopsy results in liver failure patients with renal dysfunction: a new look to combined liver kidney allocation in the post-MELD era. Transplantation 2008;86:1548-1553.
44. Fehr T, Rusi B, Fischer A, Hopfer H, Wuthrich RP, Gaspert A. Rituximab and intravenous immunoglobulin treatment of chronic antibody-mediated kidney allograft rejection. Transplantation 2009;87:1837-1841.
45. Newell KA, Asare A, Kirk AD, Gisler TD, Bourcier K, Suthanthiran M et al. Identification of a B cell signature associated with renal transplant tolerance in humans. J Clin Invest 2010;120:1836-1847.
46. Lee KM, Stott RT, Zhao G, SooHoo J, Xiong W, Lian MM et al. TGF-β-producing regulatory B cells induce regulatory T cells and promote transplantation tolerance. Eur J Immunol 2014;44:1728-1736.
47. Allison SJ. Fibrosis: Regulation of fibrotic signalling by TGF-[beta] receptor tyrosine phosphorylation. Nat Rev Nephrol 2014;10:484-484.

Figures

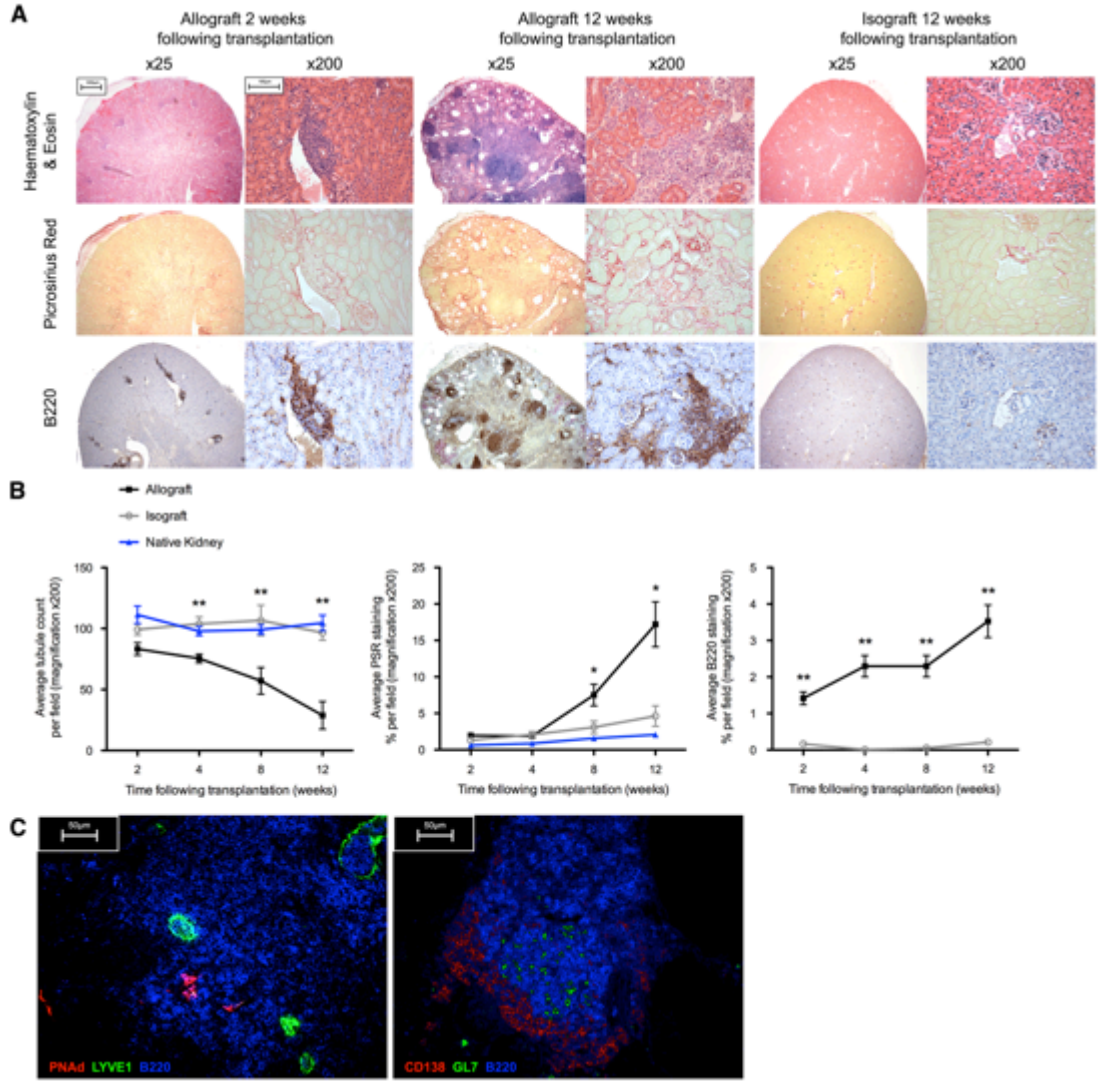

Figure 1: B cells accumulate within transplanted kidneys undergoing chronic allograft damage (CAD)(C57BL/6^{BM12}⇨C57BL/6).

(A) Representative histology of paraffin-embedded allograft transplant kidney sections. Haemotoxylin and eosin for tissue architecture, collagen with picrosirius red (red), B220^{+} B cells (brown). (B) Quantification of the number of tubules, density of collagen and B cells in transplanted kidneys. Ten micrographs at x200 magnification were analyzed (n=6 mean (SEM), ANOVA and Bonferonni *post hoc* between groups at time points. *p<0.05; **p<0.01). (C) Definition of CAD B cell infiltrates 12 weeks post transplantation in immunofluorescent micrographs identifying GL7^{+} germinal centres and CD138^{+} plasma cells, and tertiary lymphoid tissue development with PNAd^{+} high endothelial venules and LYVE1^{+} lymphatic vessels.

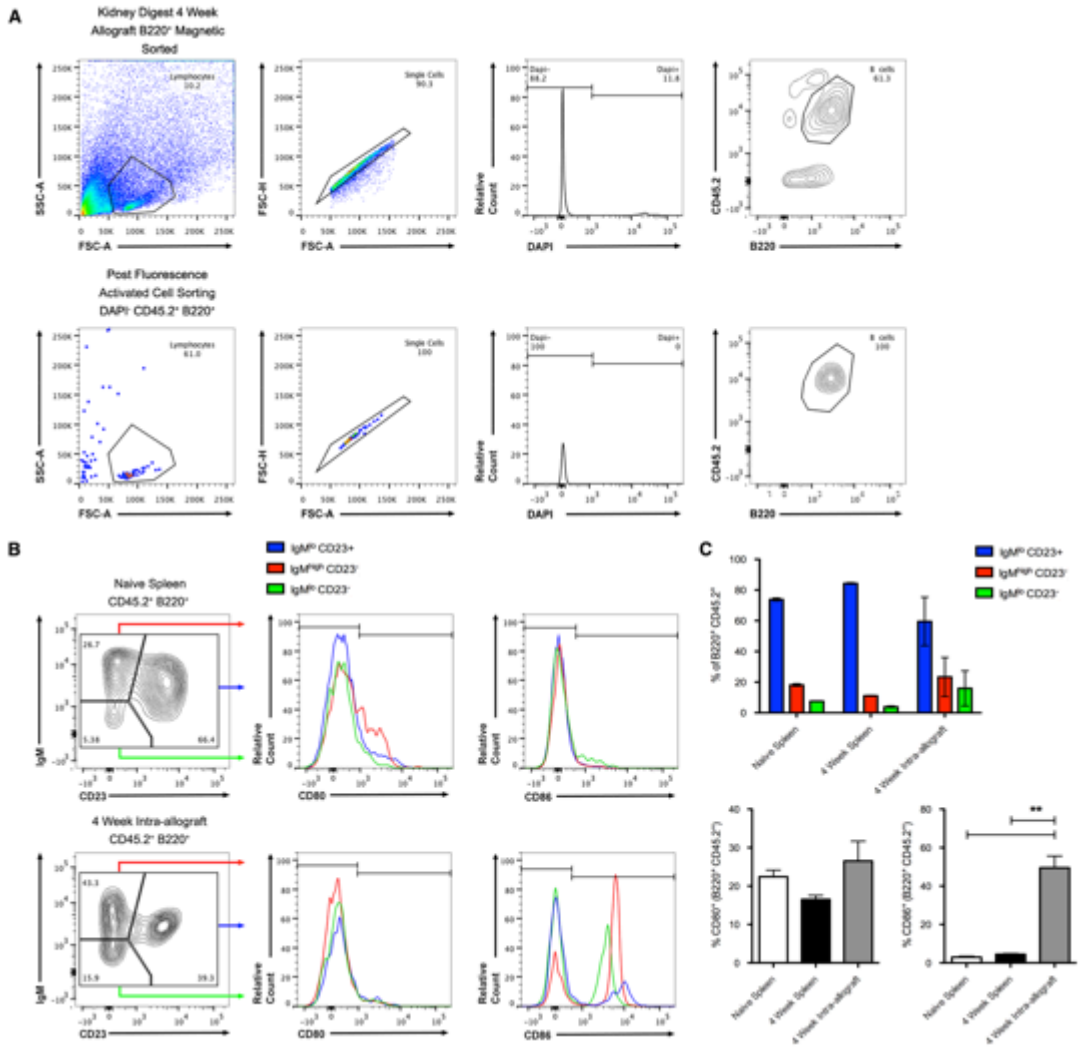

Figure 2: The phenotype of allograft (C57BL/6^{BM12}⇨C57BL/6) B cells by flow cytometry. (A) Gating of B cells from allograft kidney digest. Intra-allograft B cells isolated following allograft kidney digestion then B220^{+} magnetic bead enrichment prior to fluorescence activated cell sorting by B220^{+} CD45.2^{+} DAPI^{-} for mRNA extraction and cell culture experiments. (B) CAD intra-allograft B cell phenotype were analysed on flow cytometry and compared to naive spleen B cells. (C) Frequency of gated B cells (n=6, mean (SEM), ANOVA and Bonferonni *post hoc* between groups. **p<0.01).

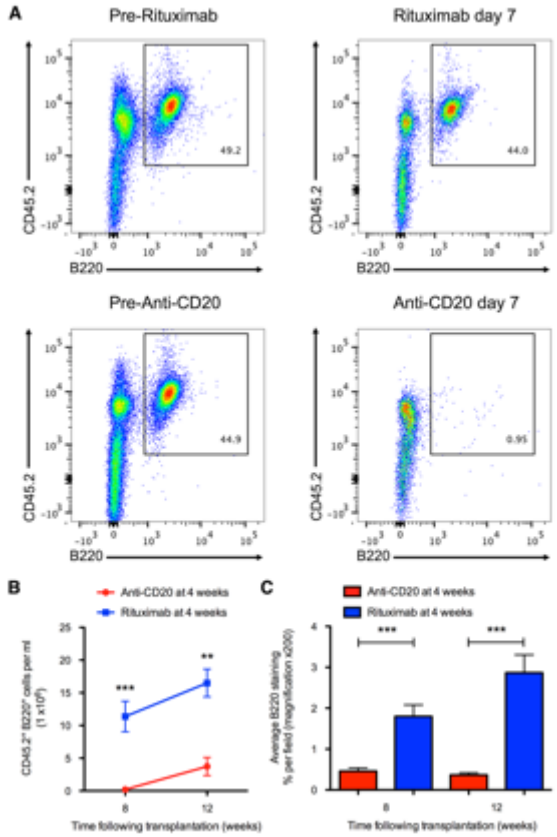

Figure 3: Anti-CD20 after transplantation depletes intra-renal B cells in chronic allograft damage (C57BL/6^{BM12}⇨C57BL/6).

(A) Flow cytometry gating of blood B cells prior to and following anti-mouse anti-CD20 or anti-human anti-CD20 (Rituximab). (B) Absolute count of blood B cells were determined in mice treated prior to, or 4 weeks after, transplantation (n=6, mean (SEM), ANOVA and Bonferonni *post hoc* between groups at single time points. **p<0.01; ***p<0.001). (C) Quantification of the immunohistochemistry micrographs of allograft density of B220^{+} B cells following anti-mouse anti-CD20 or anti-human anti-CD20 (Rituximab). Ten micrographs at x200 magnification were analyzed (n=6 mean (SEM), Mann-Whitney U test. ***p<0.001).

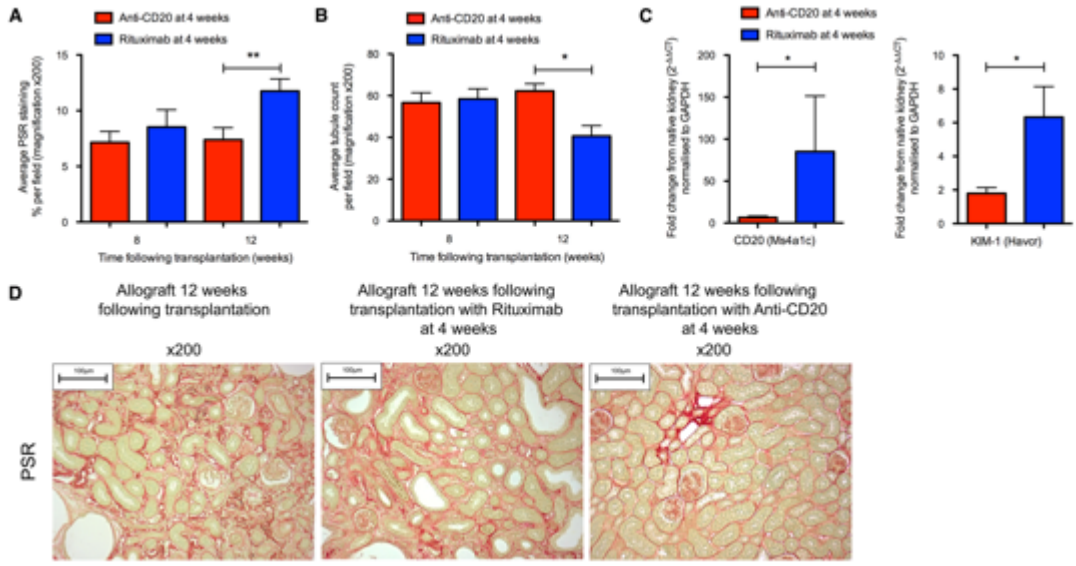

Figure 4: B cell depletion reduces chronic allograft damage (C57BL/6^{BM12}⇨C57BL/6).
(A) Quantification of allograft density of collagen following picrosirius red staining following anti-mouse anti-CD20 or anti-human anti-CD20 (Rituximab). (B) Quantification of the number of tubules by haemotoxylin and eosin staining following treatment. Ten micrographs at x200 magnification were analyzed (n=6, mean (SEM), Mann-Whitney U test between groups at single time points. *p<0.05; **p<0.01). (C) Allografts at 8 weeks after transplantation from mice depleted at 4 weeks of B cells had a decreased expression of CD20 and Kim-1 mRNA (n=8, assay in triplicate, mean (SEM), Mann-Whitney U test. *p<0.05). (D) Representative histology of paraffin-embedded transplant kidney sections. Fibrosis identified by collagen with picrosirius red, tubular atrophy demonstrated in untreated and placebo treated tissue.

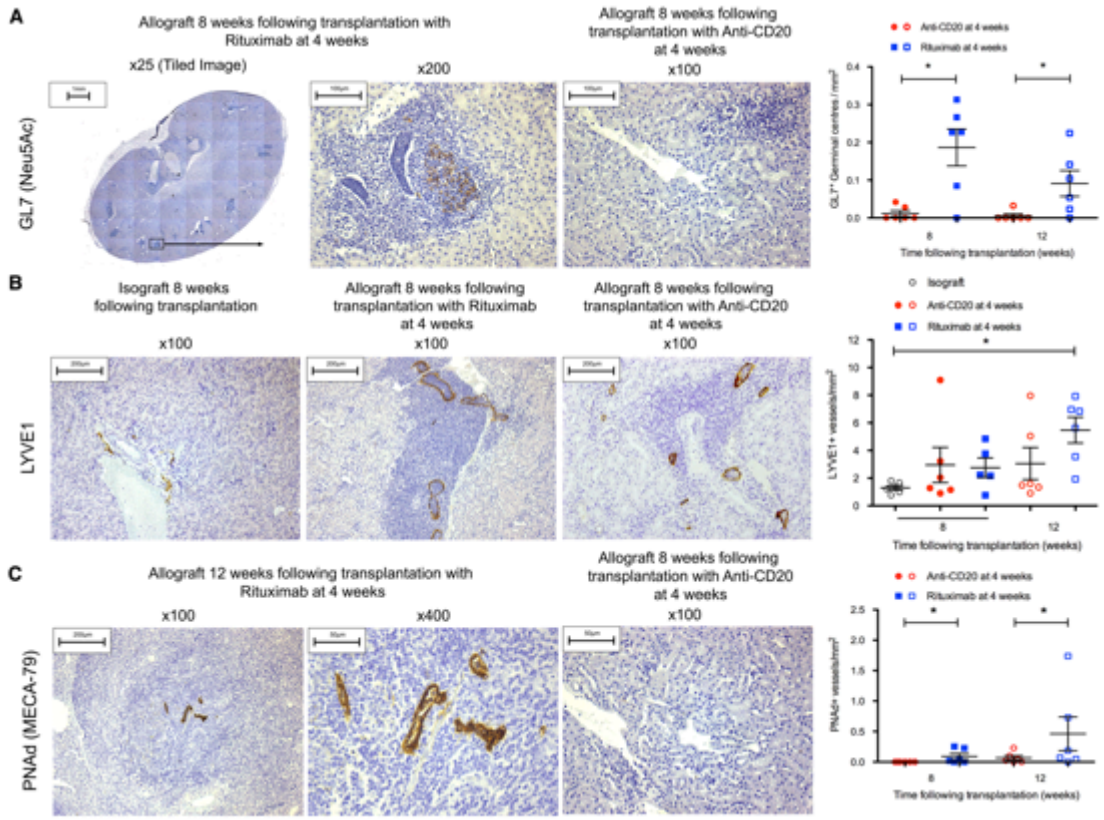

Figure 5: Reduction in tertiary lymphoid tissue development.

(**A**) Representative immunohistochemistry of $GL7^+$ germinal centres (brown) counted per total tissue area section. (**B**) Absolute numbers of $LYVE1^+$ lymphatic vessels (brown) per total tissue area section. (**C**) Absolute numbers of $PNAd^+$ high endothelial venules (brown) per total tissue area section in anti-CD20 or placebo (Rituximab) treated allograft kidneys (n=6, mean (SEM), Mann-Whitney U test. *$p<0.05$).

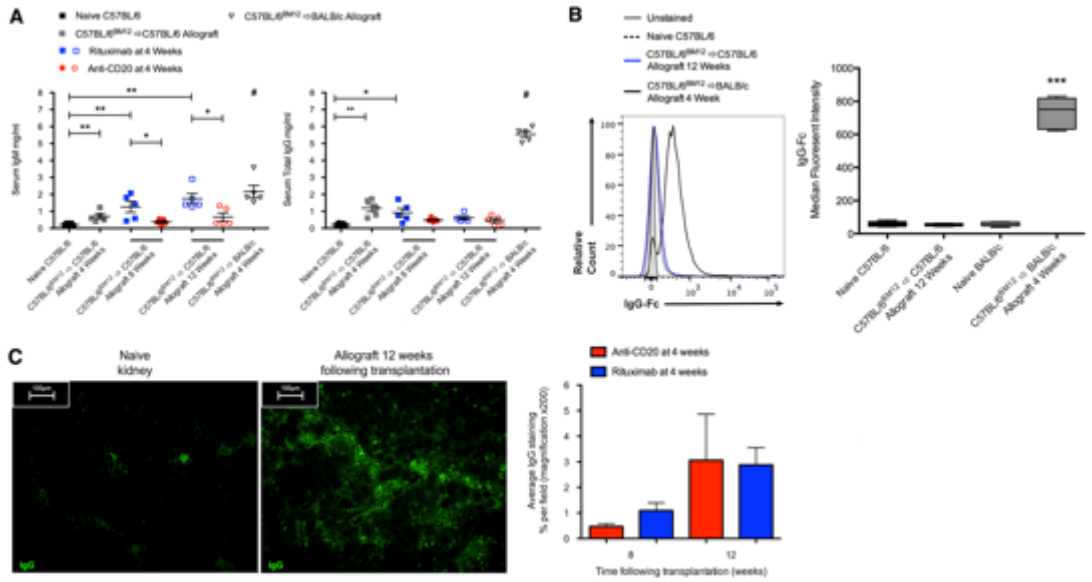

Figure 6: CAD is not primarily mediated by donor-specific immunoglobulin.
C57BL/6^{BM12} donor kidneys transplanted in to **C57BL/6 allograft** recipients (C57BL/6^{BM12}⇨C57BL/6) or **BALBc allograft** recipients (C57BL/6^{BM12}⇨BALB/c). (A) Serum concentrations of IgM and total IgG from naïve and transplant recipient mice were measured (see supplemental table 1 for absolute values)(n=5, assay in duplicate, mean (SEM), ANOVA and Bonferonni *post hoc* between groups. *p<0.05; **p<0.01; ♯p<0.001 against all groups). (B) Flow cytometry of live splenocytes incubated with transplant recipient serum to detect donor-specific IgG, quantification by median fluorescent intensity (n=6, assay in triplicate, error bars median and interquartile-range, ANOVA and Bonferonni *post hoc* between groups. ***p<0.001). (C) Intra-allograft IgG content with representative immunofluorescence comparing naïve kidney and of CAD allograft 12 weeks post-transplantation demonstrating deposited IgG (green) and B cells bearing IgG. Quantification of IgG+ micrographs following treatment (n=6, mean ± SEM, Mann-Whitney U test, N.S.).

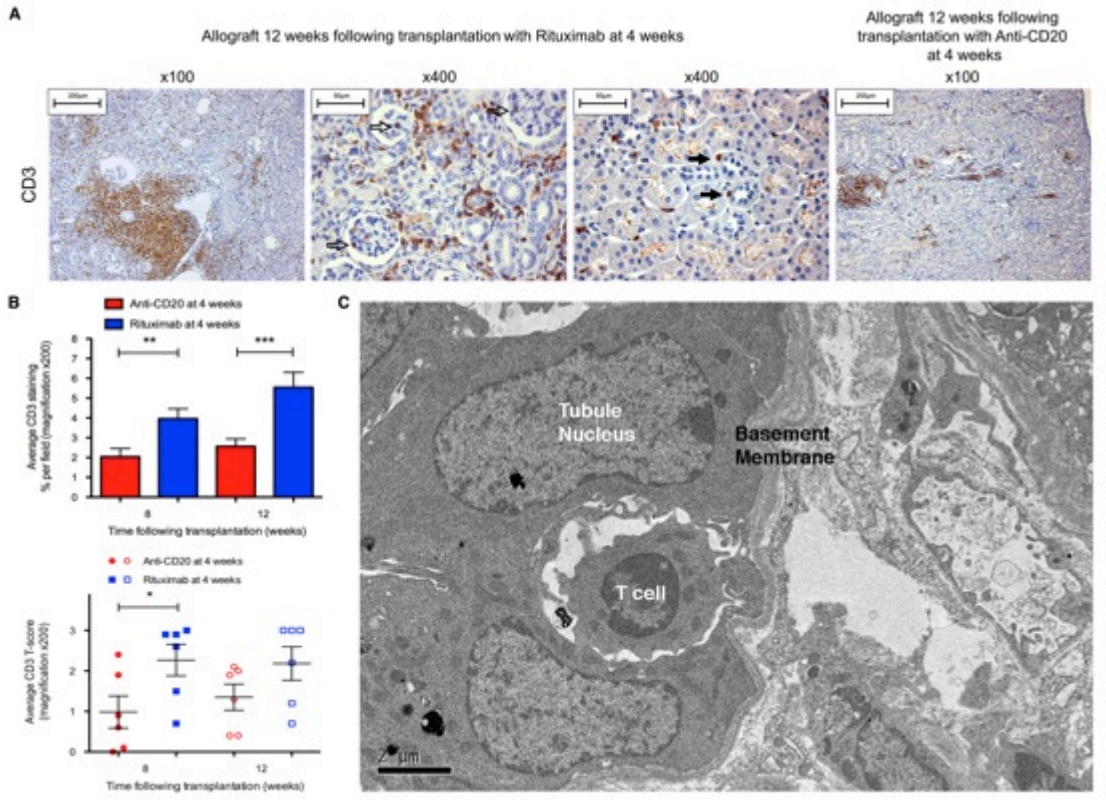

Figure 7: B cell depletion reduces T cell accumulation.

(A) Representative immunohistochemistry of $CD3^+$ infiltrating T cells (brown). T cells identified invading glomeruli (hollow arrows) and tubules (block arrows). (B) Quantification of the immunohistochemistry micrographs to determine allograft density of $CD3^+$ T cells in anti-CD20 or placebo treated (Rituximab). Pathological grading (T-score) of allografts treated at four weeks. Ten micrographs at x200 magnification were analyzed (n=6, mean (SEM), Mann-Whitney U test. *p<0.05; **p<0.01; ***p<0.001). (C) Transmission electron microscopy image of CAD kidney at 8 weeks post transplantation. T cell can be identified breaching the basement membrane and invading the renal tubule.

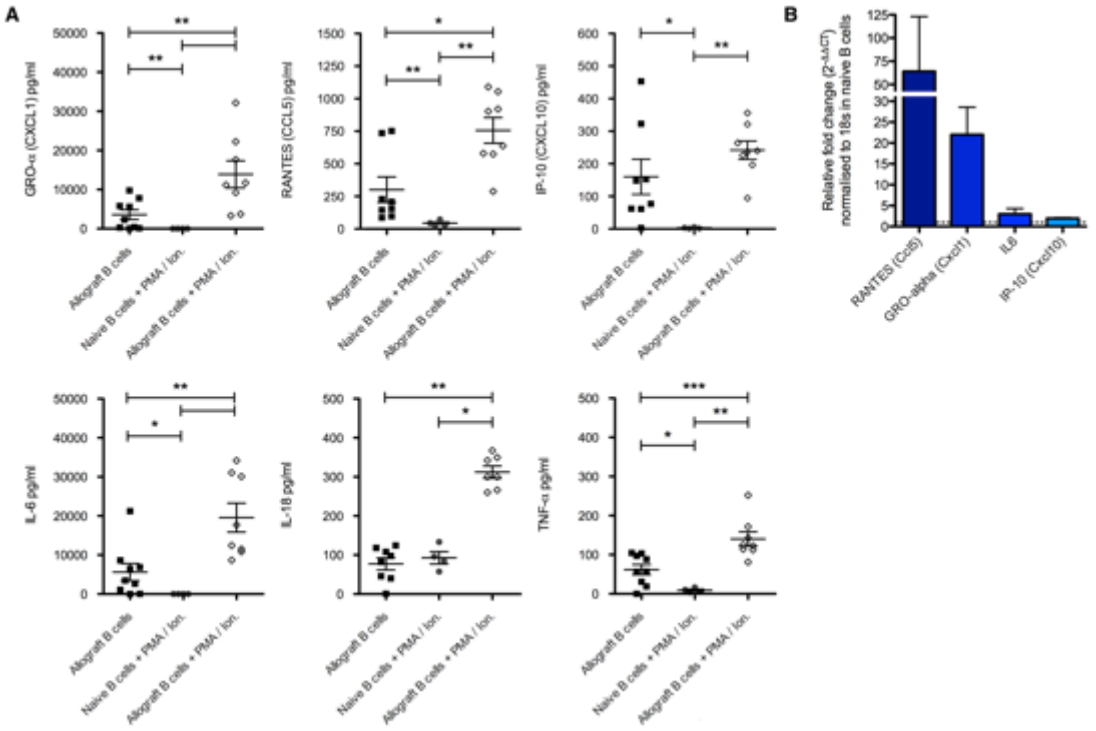

Figure 8: B cells secrete fibrosis related cytokines.

(A) Cytokine supernatant assay of isolated allograft (C57BL/6^{BM12}⇨C57BL/6) B cells cultured for 72 hours alone or ionomycin (Ion.) and phorbitol mysirate (PMA) and compared to stimulated naïve B cells (n=6, mean (SEM), ANOVA and Bonferonni *post hoc* between pairs of groups. *p<0.05; **p<0.01; ***p<0.001). (B) Comparative quantification of mRNA fold difference by qRT-PCR in isolated allograft B cells compared to naïve spleen B cells, genes of interest normalized to two genes with 18s represented (n=8, assay in triplicate).

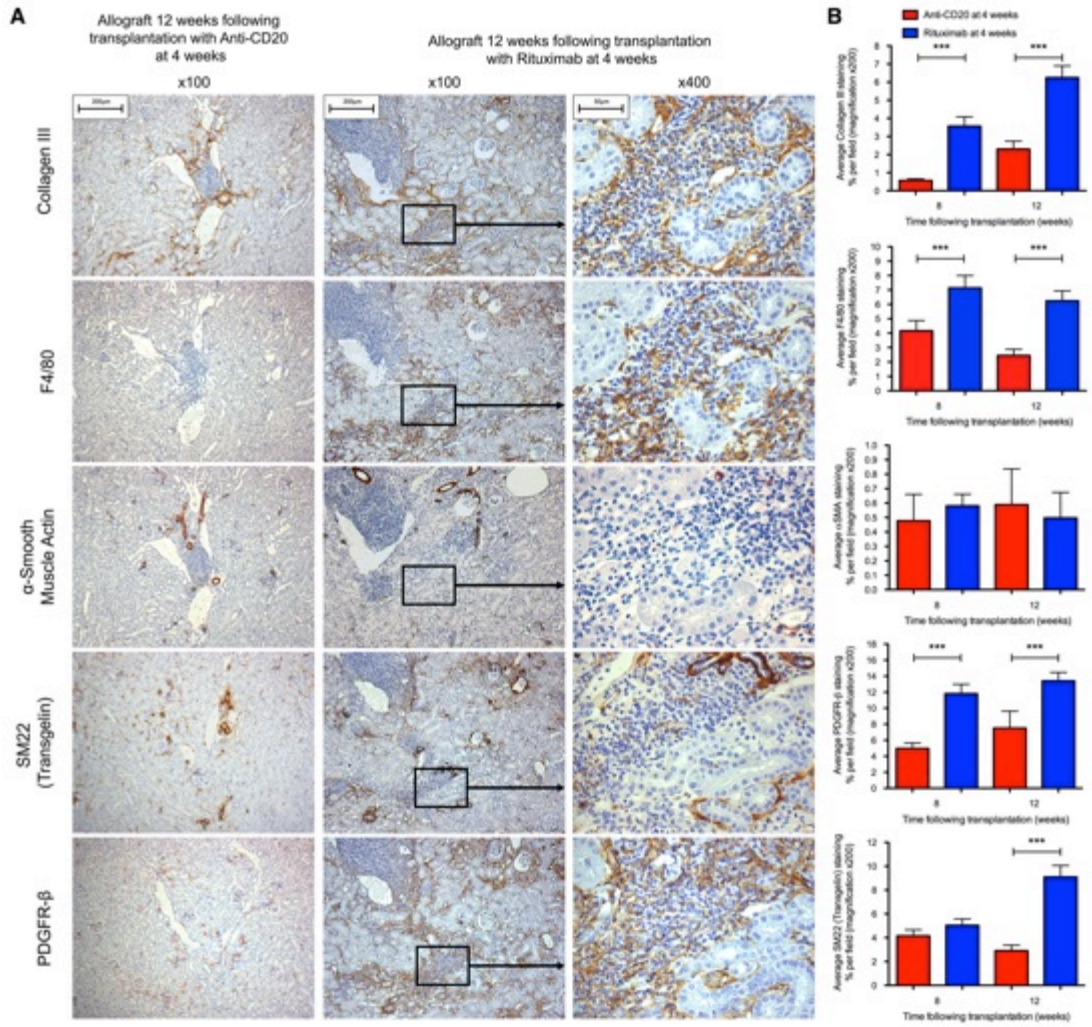

Figure 9: Reduced fibrosis is associated with fewer macrophage and fibroblasts in the allograft (C57BL/6^{BM12}⇨C57BL/6).

(A) Representative immunohistochemistry of serial sections for type III collagen, F4/80, α-Smooth Muscle Actin (α-SMA), SM22 (transgelin) and platelet derived growth factor receptor-β (PDGFR-β). (B) Quantification of type III collagen, F4/80^{+} mononuclear cell infiltration, presence of α-SMA^{+} myofibroblast, PDGFR-β^{+} or transgelin^{+} fibroblast-like cells in anti-CD20 or placebo (Rituximab) treated allograft treated at four weeks. Ten micrographs at x200 magnification were analyzed (n=6, mean (SEM), Mann-Whitney U test. ***p<0.001).

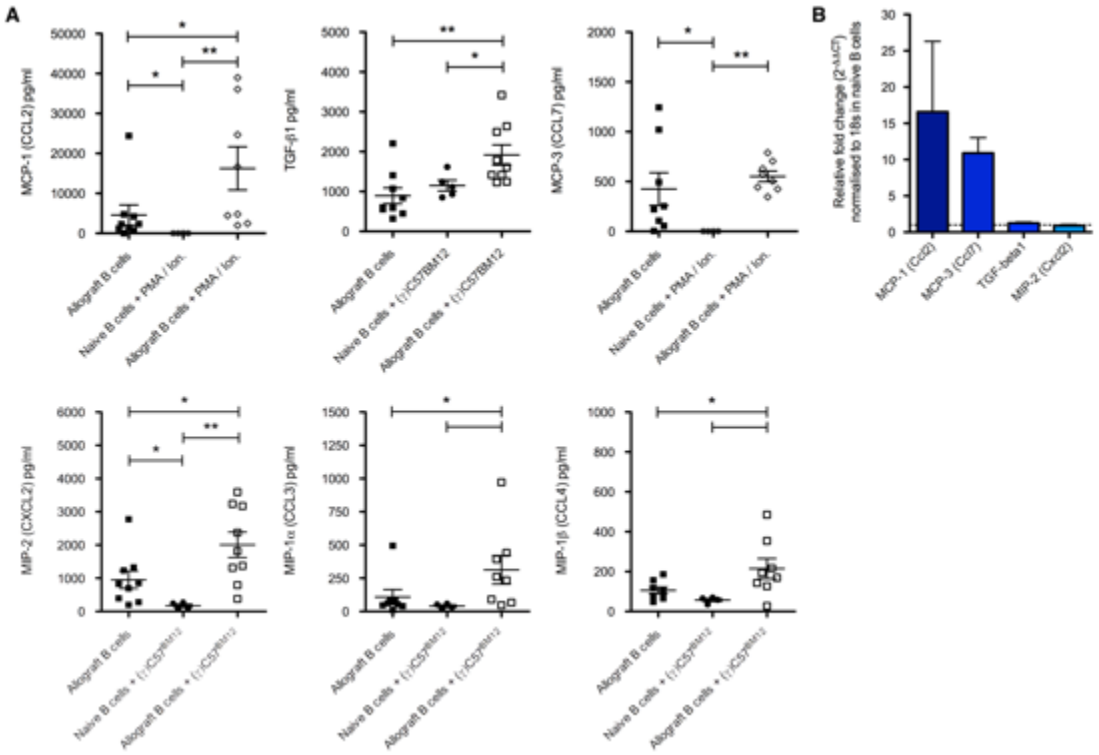

Figure 10: B cells secrete profibrotic cytokines.

(A) Cytokine supernatant assay of isolated allograft (C57BL/6^{BM12}⇨C57BL/6) B cells cultured for 72 hours alone in media or ionomycin (Ion.) and phorbitol mysirate (PMA) or with γ-irradiated C57BL/6^{BM12} splenocytes and compared to stimulated naïve B cells (n=6-8, assay in duplicate, mean (SEM), ANOVA and Bonferonni *post hoc* between pairs of groups. *p<0.05; **p<0.01). (B) Comparative quantification of mRNA fold difference by qRT-PCR in isolated allograft B cells compared to naïve spleen B cells, genes of interest normalized to two genes with 18s represented (n=8, assay in triplicate).

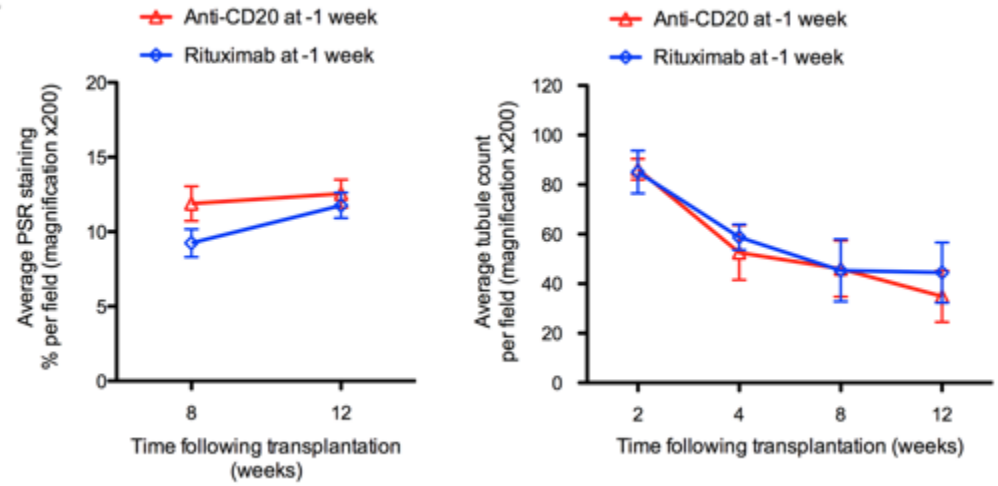

Figure S1: CAD (C57BL/6^{BM12}⇨C57BL/6) is not altered by B cell depletion prior to transplantation.

Quantification of allograft density of collagen following picrosirius red staining following anti-mouse anti-CD20 or anti-human anti-CD20 (Rituximab) 1 week prior to transplantation. Quantification of the number of tubules by haemotoxylin and eosin staining following treatment. Ten micrographs at x200 magnification were analyzed (n=6, mean (SEM), ANOVA and Bonferonni *post hoc* between pairs of groups. N.S.).

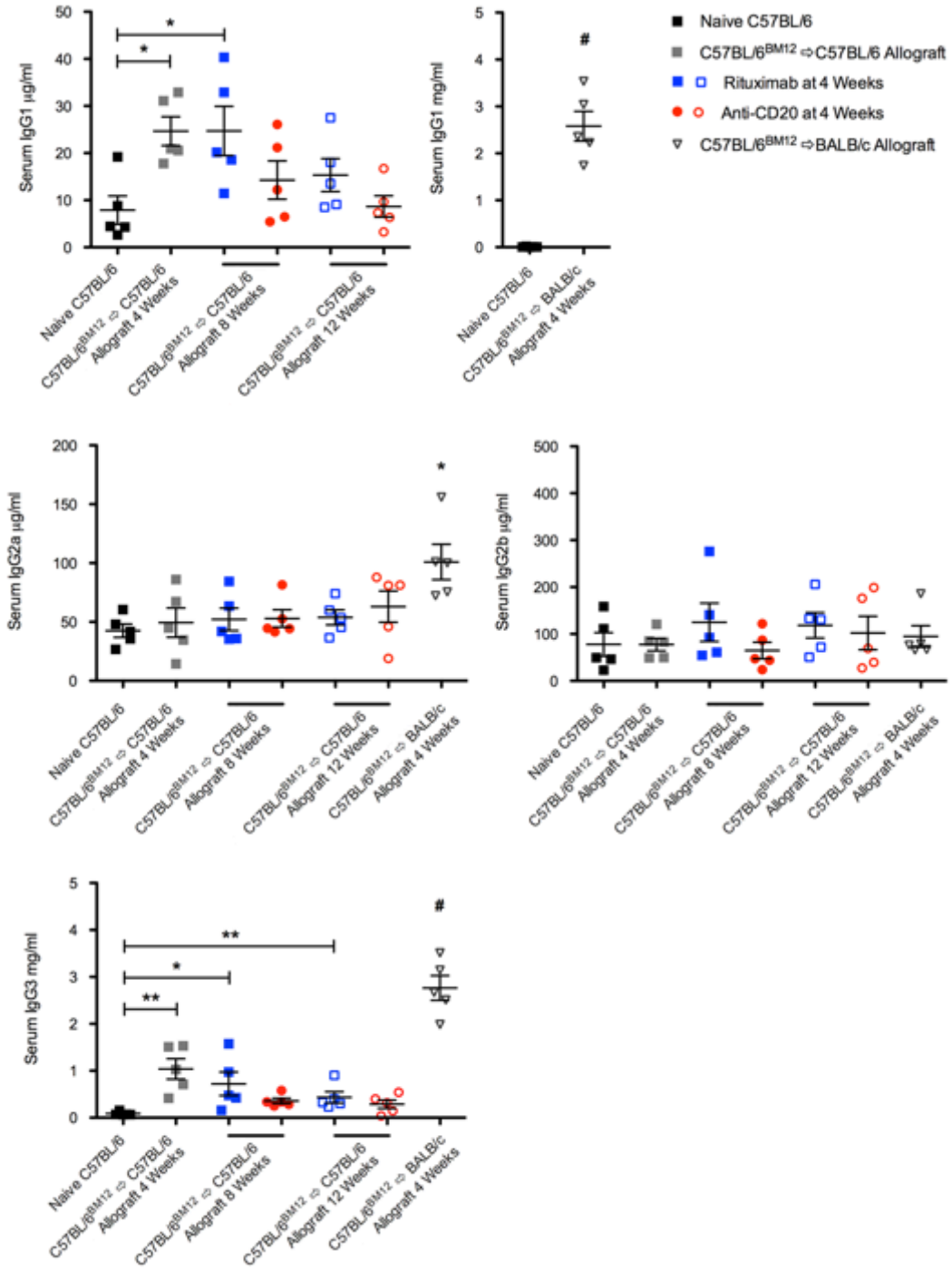

Figure S2: Serum concentration of IgG subclasses.

C57BL/6^{BM12} donor kidneys transplanted in to C57BL/6 allograft recipients (C57BL/6^{BM12}⇨C57BL/6) or BALBc allograft recipients (C57BL/6^{BM12}⇨BALB/c). Serum concentration of IgG subclasses from naïve and transplant recipient mice were measured (see **Supplemental Table S1** for absolute values)(n=5, assay in duplicate, mean (SEM), ANOVA and Bonferonni *post hoc* between pairs of groups. *p<0.05; **p<0.01; ♯p<0.001 against all groups).

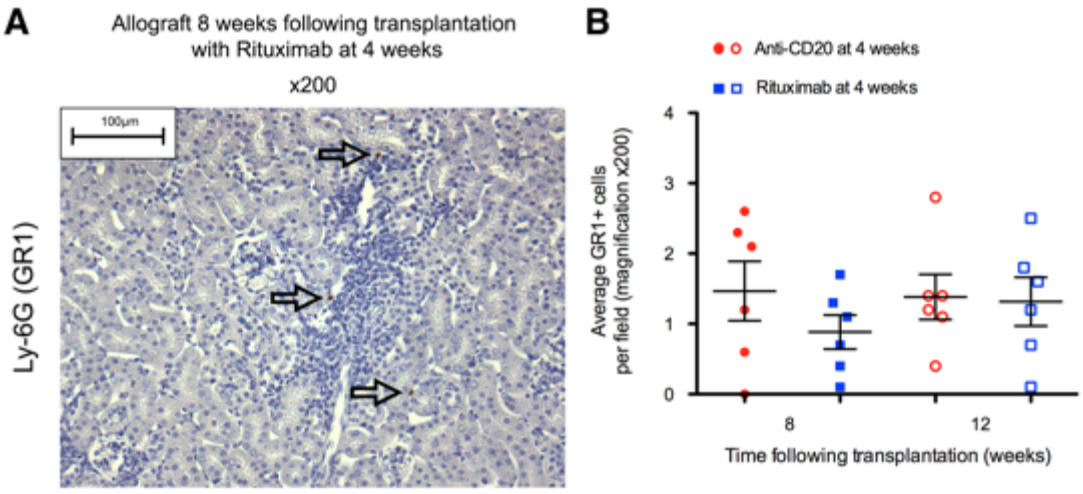

Figure S3: B cell depletion did not effect allograft (C57BL/6^{BM12}⇨C57BL/6) neutrophil infiltration.

(A) Intra-allograft Gr1^{+} neutrophils (hollow arrows) identified on immunohistochemistry (brown). (B). Quantification of the immunohistochemistry micrographs of allograft Gr1^{+} neutrophils following treatment, ten micrographs at x200 magnification were analyzed (n=6, mean (SEM), ANOVA followed by Mann-Whitney U test. N.S).